JOURNAL OF GEOPHYSICAL RESEARCH, VOL. 105, NO. D7, PAGES 9303–9320, APRIL 16, 2000

Perturbation dynamics in atmospheric chemistry

Brian F. Farrell

Department of Earth and Planetary Sciences, Harvard University, Cambridge, Massachusetts

Petros J. Ioannou

Department of Physics, National and Capodistrian University of Athens, Athens

Abstract. Current understanding of how chemical sources and sinks in the atmosphere interact with the physical processes of advection and diffusion to produce local and global distributions of constituents is based primarily on analysis of chemical models. One example of an application of chemical models which has important implications for global change is to the problem of determining sensitivity of chemical equilibria to changes in natural and anthropogenic sources. This sensitivity to perturbation is often summarized by quantities such as a mean lifetime of a chemical species estimated from reservoir turnover time or the decay rate of the least damped normal mode of the species obtained from eigenanalysis of the linear perturbation equations. However, the decay rate of the least damped normal mode or a mean lifetime does not comprehensively reveal the response of a system to perturbation. In this work, sensitivity to perturbations of chemical equilibria is assessed in a comprehensive manner through analysis of the system propagator. When chemical perturbations are measured using the proper linear norms, it is found that the greatest disturbance to chemical equilibrium is achieved by introducing a single chemical species at a single location, and that this optimal perturbation can be easily found by a single integration of the transpose of the dynamical system. Among other results are determination of species distributions produced by impulsive, constant, and stochastic forcing; release sites producing the greatest and least perturbation in a chosen constituent at another chosen site; and a critical assessment of chemical lifetime measures. These results are general and apply to any perturbation chemical model, including three-dimensional global models, provided the perturbations are sufficiently small that the perturbation dynamics are linear.

1. Introduction

Models commonly used to assess the impact of perturbations to the chemical constituents of the atmosphere consist of continuity equations in which the time derivatives of the number densities of chemical species at grid points are related by terms representing advection, diffusion, sources, sinks, and reactions among the species. Given an initial state such a model can be integrated in time to obtain the species number densities as a function of the spatial and temporal distribution of sources. Although chemical equilibria are, in general, nonlinear, the response of the nonlinear equilibrium to sufficiently small perturbations is intrinsically linear, and even if the expected perturbations are large enough to require nonlinear terms in a comprehensive perturbation analysis, still a thorough understanding of the linear dynamics of small perturbations is a necessary foundation for this extension into the nonlinear regime. Therefore we assume in this work that the model is linear in the perturbations or can be linearized about a representative equilibrium state. For a description of such models, see the work of *Khalil and Rasmussen* [1984], *Chameides and Perdue* [1997], and *Prather* [1996, 1997, 1998]. Prather showed that the evolution of chemical perturbations to stationary equilibrium states can be obtained by decomposing the perturbation into the natural modes (the eigenvectors) of the linear system and that the least damped natural mode is the pattern that eventually dominates the response to any initial perturbation. He also noted that this asymptotic response is often masked by the presence of the other natural modes that are also excited by the initial perturbation and which interfere on superposition, leading to transient excursions of chemical per-

Paper number 1999JD901021.
0148-0227/00/1999JD901021$09.00

turbations, a phenomenon ascribed to the "nonorthogonality" of the modes. In light of the insights proceeding from application of the method of modes, identification of the natural modes in atmospheric chemical transport models has been advanced as the preferred method for describing the complex evolution of chemical perturbations [*Prather*, 1998].

However, systematic analysis of perturbation dynamics in chemical systems immediately encounters an impediment in making precise the concept of orthogonality among the natural modes. The familiar dot product allows both defining an angle between vectors as well as associating a length to each vector, and if chemical perturbations, described by the vector $\mathbf{x}$, are measured by their euclidean length (otherwise called the L_2 norm), then the concept of orthogonality among chemical perturbations and among the normal modes of the system is definable and the transient growth of perturbations, in the L_2 sense, can be related to the orthogonality of the modes. A perturbation imposed on a stable system with orthogonal eigenvectors necessarily decays as measured in the L_2 norm at a rate faster than the decay rate of the least damped mode, and this limiting decay rate is approached asymptotically with time. (A system is stable if the real parts of its eigenvalues are negative.) For stable systems with nonorthogonal eigenvectors a perturbation measured in L_2 is not assured to decay at all times and may, in fact, increase for a period of time before eventually assuming its asymptotic decay rate, which is that of the least damped mode.

However suggestive these L_2 measures may be, chemical perturbations can only be sensibly assessed with a measure based on the number of molecules, and while such linear measures (as opposed to quadratic, e.g., L_2 measures) associate length to vectors, they do not allow definition of an angle between vectors. Nevertheless, while the concept of orthogonality is lost in these measures, the concept of projection of a perturbation onto eigenvectors remains valid, and the evolution of the perturbation still can be viewed in terms of summation over the evolving eigenvectors.

In order to understand the implications of this distinction between linear and quadratic measures, consider the abstract linear equation assumed to govern evolution of chemical constituents in a hypothetical chemical model:

$$\frac{d\mathbf{x}}{dt} = \mathbf{A}\mathbf{x} \,, \tag{1}$$

where $\mathbf{A}$ is a real matrix and $\mathbf{x}$ is a vector containing as its entries the abundance of the chemical constituents in the model collocated at grid points. Associated with $\mathbf{A}$ is the transpose matrix $\mathbf{A}^T$. There is an intimate relation between the eigenvectors of these two matrices: the eigenvectors of $\mathbf{A}^T$ arranged in rows form the projection matrix that determines the coefficients of projection of a perturbation on the eigenvectors of $\mathbf{A}$. (If $\mathbf{U}$ are the eigenvectors of $\mathbf{A}$ arranged as columns, then the eigenvectors of $\mathbf{A}^T$ are $(\mathbf{U}^{-1})^T$. A vector $\mathbf{x}$ can be written as $\mathbf{x} = \mathbf{U}(\mathbf{U}^{-1}\mathbf{x})$, where $\mathbf{U}^{-1}\mathbf{x}$ is recognized as the coefficients of projection of the vector on the eigenvectors. The matrix $\mathbf{U}^{-1^T}$ is called the bi-orthogonal matrix. If $\mathbf{u}$ is a specific eigenvector of $\mathbf{A}$ corresponding to a given column $\mathbf{U}$, then its bi-orthogonal is the corresponding column of the bi-orthogonal matrix.) If the eigenvectors of $\mathbf{A}$ and $\mathbf{A}^T$ are the same, then the two matrices commute; that is, $\mathbf{A}\mathbf{A}^T - \mathbf{A}^T\mathbf{A} = 0$, and the system matrix $\mathbf{A}$ is called normal, otherwise nonnormal. In the chemical literature, where discretization of linear operators usually results in a real matrix, nonnormality of $\mathbf{A}$ can be expected when the matrix $\mathbf{A}$ exhibits asymmetry about the diagonal. (However, even for real matrices, nonnormality is not equivalent to asymmetry of the entries about the diagonal. Consider the orthogonal matrices which are asymmetric but nevertheless have the same bi-orthogonal and eigenvector matrices.)

Nonnormality of the system matrix $\mathbf{A}$ indicates that the eigenvalues and eigenvectors of the system may be illconditioned and highly sensitive to small perturbations in the parameters of the system [*Trefethen*, 1991]. As a result, projection on the natural modes may be illconditioned unless the parameters of the system are known with great certainty.

However, while nonnormality of the system identifies the potential for L_2 growth, accurate assessment of growth in other measures, such as the linear measures appropriate in chemistry, must proceed from detailed calculation in the measure selected. This can be done by defining carefully the measure of chemical perturbations and then determining the maximum chemical perturbation that can be achieved at any time in this measure. This task is facilitated by shifting attention from natural modes to the propagator (introduced in the next paragraph), which can reveal directly the perturbation dynamics of the system.

The temporal evolution of an arbitrary system of finite dimension can be expressed as

$$\mathbf{x}(t) = \mathbf{\Phi}(t)\,\mathbf{x}(0) \,, \tag{2}$$

where $\mathbf{\Phi}(t)$ is the propagator, which in the case of a time-independent system is the matrix exponential $e^{\mathbf{A}t}$. (The matrix exponential $e^{\mathbf{A}t}$ is defined as $e^{\mathbf{A}t} = \mathbf{I} + \mathbf{A}t + \mathbf{A}^2t^2/2! + \cdots$. There are efficient algorithms available for direct evaluation of the matrix exponential that do not require prior eigenanalysis of $\mathbf{A}$. We use a Padé approximation routine with scaling and squaring described in chapter 11.3 of *Golub and Van Loan* [1996].)

We wish to determine the initial perturbation producing the greatest perturbation growth over a specified interval of time (this perturbation is called the optimal perturbation). This initial perturbation can be obtained directly from analysis of the propagator, and it does not, in general, coincide with a particular mode of the system.

The optimal growth over time t is given by the norm of the propagator $||\mathbf{\Phi}(t)||$, which is defined to be the maximum measure of $\mathbf{x}(t)$ over all initial unit pertur-

bations $\mathbf{x}(0)$ (the measures used at the initial and final times need not be the same). In the meteorological literature a systematic theory has been developed for identifying optimal perturbations in the L_2 norm [*Farrell*, 1988; *Farrell and Ioannou*, 1996a,b], but a comparable theory has not been advanced for chemical perturbations. As discussed above, the theory developed in meteorology can not be carried over directly to chemistry, because of the inherent distinction between the measure of perturbations in dynamical systems (the energy of perturbations), which is quadratic and associated with an L_2 norm, and the measure in chemical systems (the number of molecules), which is linear. (There is a notable exception: if we choose to measure the final perturbations only at a specific location, then the linear measure gives the same values as are obtained with the L_2 norm. In these cases the results available for analysis of nonnormal systems with L_2 norms [*Farrell and Ioannou*, 1996a] are directly applicable.) It turns out, however, that the linearity of the appropriate measure in chemical systems is, in fact, an advantage that leads to a particularly efficient method for obtaining optimal initial conditions. In the sequel the appropriate measure of chemical perturbations is introduced, and the theory for obtaining optimal perturbations to chemical systems is developed.

In order to streamline the development we will limit the analysis to time-independent systems, for which the propagator is the matrix exponential $\mathbf{\Phi(t)} = e^{\mathbf{At}}$. The analysis can be carried over, with minor modifications, to time-dependent systems.(The system propagator for a time-dependent system can be obtained by forward integration of the identity matrix. We note that eigenanalysis is not defined for time-dependent systems, so that methods of analysis based on eigenmodes can not be extended to apply to time-dependent systems.)

A simple atmospheric chemical system consisting of the advection, diffusion, loss, and interaction of CH_3Br and Br_y in a one-dimensional atmospheric column is taken as an example (the example is based on the B1 model of *Prather* [1977]). We apply to this system the methods of nonnormal analysis and obtain general properties of the solution including the response of the system to forcing applied impulsively, continuously, and stochastically distributed in space and time: the perturbations most effective in disturbing the chemical equilibrium and appropriate measures of timescale for this system. Before presenting the theory we describe the example chemical system.

2. CH_3Br/Br_y Perturbation Dynamics

The mixing ratios of a species, denoted χ_i, satisfy the advection equation [*Brasseur and Solomon*, 1986; *Andrews et al.*, 1987]:

$$\frac{\partial \chi_i}{\partial t} + \vec{\mathbf{u}} \cdot \nabla \chi_i = S \,, \tag{3}$$

where $\vec{\mathbf{u}}$ is the velocity field and S denotes the net sources. Consider a model of the ascending branch of the Hadley circulation at the equator. Zonal homogeneity and symmetry about the equator imply that the horizontal derivatives vanish. The advection equation that governs evolution of mixing ratios of the chemical constituents with height and time reduces under these assumptions to

$$\frac{\partial \chi_i}{\partial t} + w(z) \frac{\partial \chi_i}{\partial z} = S \,. \tag{4}$$

Using (4), evolution of number densities in the coupled CH_3Br/Br_y system satisfies the following equations:

$$\frac{dn_{CH_3Br}}{dt} = - w(z)N(z) \frac{d}{dz}\left[n_{CH_3Br}/N(z)\right] + \\ + \frac{d}{dz}\left\{K(z)N(z) \frac{d}{dz}\left[n_{CH_3Br}/N(z)\right]\right\} - \\ - m_1(z)\, n_{CH_3Br} + P_{CH_3Br}, \tag{5a}$$

$$\frac{dn_{Br_y}}{dt} = - w(z)N(z) \frac{d}{dz}\left[n_{Br_y}/N(z)\right] + \\ + m_1(z)\, n_{CH_3Br} - m_2(z)\, n_{Br_y} + \\ + \frac{d}{dz}\left\{K(z)N(z) \frac{d}{dz}\left[n_{Br_y}/N(z)\right]\right\} . \tag{5b}$$

Here z is the height, n_i is the number density (m^{-3}) of species i, and $N(z)$ is the atmospheric number density (m^{-3}). The source of CH_3Br is P_{CH_3Br} (m^{-3} s^{-1}), which may vary both in space and in time. The chemistry is as in the *Prather* [1997] B1 model. The CH_3Br is destroyed at a rate $m_1(z)$ by reacting with OH in the troposphere ($z < 10$ km) and by photolysis in the stratosphere. The bromine species, collectively denoted by Br_y, are formed from the destruction of CH_3Br and rained out at a rate $m_2(z)$ in the troposphere. The vertical distribution of $m_1(z)$ and $m_2(z)$ is shown in Figure 1a. The eddy diffusion coefficient is denoted by K. The first term on the right hand side of (5a) and (5b) represents vertical advection by the mass-conserving velocity field. The distributions with height of the vertical velocity $w(z)$ and of the diffusion coefficient $K(z)$ are shown in Figure 1b.

The continuity equations for the number density tendencies (equations (5a) and (5b)) are collocated at equally spaced levels in z, and the spatial differential operators are approximated with second-order difference operators. The number of collocation points N is chosen such that the solutions are converged to the continuous system (typically 60 levels are adequate).

Equations (5a) and (5b) are written in matrix form:

$$\frac{d\mathbf{n}}{dt} = \mathbf{An} + \mathbf{p}, \tag{6}$$

where $\mathbf{n}$ is the column vector of the number densities in which the first N elements are the number densities of CH_3Br in sequence from the ground to the top of the

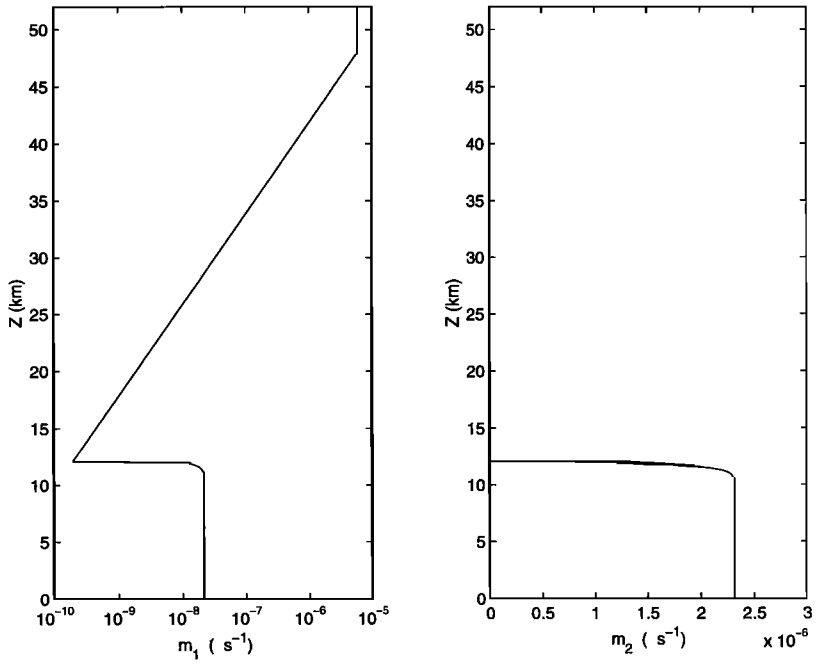

Figure 1a. (left) Chemical loss rate of CH_3Br as a function of height. The loss rate is constant in the troposphere at 2.166×10^{-8} s^{-1}; above 10 km it increases with height as $6 \times 10^{-6}\, p^{-2}$, where $p = 1000 \times 10^{-z/16}$ mbars is the pressure at height z (kilometers), and it is constant above $p = 1$ mbar. (right) Chemical loss rate of Br_y: 2.315×10^{-6} below 10 km owing to rain out, and zero elsewhere. Values are as in the work of *Prather* [1997].

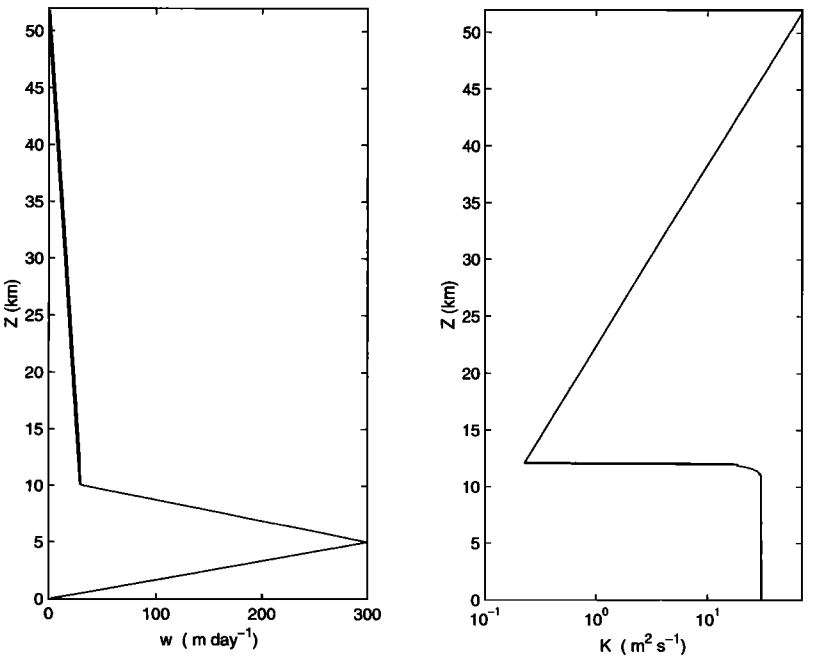

Figure 1b. (left) Vertical velocity (m d^{-1}) as a function of height (km). For $z \leq 5$, $w = 60z$, for $5 < z < 10$, $w = 300 - 54(z - 5)$, and for $z \geq 10$, $w = 30\,[1 - (z - 10)/42]$. (right) Diffusion coefficient as a function of height: $K = 30$ m^2 s^{-1} for $z < 12$, $K = 0.3$ m^2 s^{-1} at $z = 14$ km, and K increases as p_{14}/p above 14 km, where p is the atmospheric pressure and p_{14} is its value at 14 km (as in the work of *Prather* [1997]).

stratosphere (taken at 52 km), and the last N elements are the corresponding Br_y number densities. The source vector $\mathbf{p}$ is $[P, 0]^T$, as no source of Br_y is included. The matrix $\mathbf{A}$ has the form

$$\mathbf{A} = \begin{pmatrix} \mathbf{A}_{11} & \mathbf{A}_{12} \\ \mathbf{A}_{21} & \mathbf{A}_{22} \end{pmatrix}, \tag{7}$$

where all the submatrices are $N \times N$; $\mathbf{A}_{11}$ is the matrix of the discretized differential operator

$$\mathbf{A}_{11} = -w(z)N(z)\frac{d}{dz}\frac{1}{N(z)} - m_1(z) + \\ + \frac{d}{dz}\left(K(z)N(z)\frac{d}{dz}\frac{1}{N(z)}\right), \tag{8}$$

operating on $\mathbf{n}_{CH_3Br}$; $\mathbf{A}_{12}$ is zero; $\mathbf{A}_{21}$ is the diagonal matrix with the values of $m_1(z)$; and finally $\mathbf{A}_{22}$ is

$$\mathbf{A}_{22} = -w(z)N(z)\frac{d}{dz}\frac{1}{N(z)} - m_2(z) + \\ + \frac{d}{dz}\left(K(z)N(z)\frac{d}{dz}\frac{1}{N(z)}\right), \tag{9}$$

operating on $\mathbf{n}_{Br_y}$.

The state vector of the number densities at time t is given by

$$\mathbf{n}(t) = e^{\mathbf{A}t}\,\mathbf{n}(0) + \int_0^t e^{\mathbf{A}(t-s)}\,\mathbf{p}(s)\,ds, \tag{10}$$

where $\mathbf{n}(0)$ is the initial distribution of the chemical species. When all the eigenvalues of $\mathbf{A}$ are stable, i.e., have negative real part, a well-defined steady state exists which is independent of the initial distribution $\mathbf{n}(0)$. For the simple case in which the source is independent of time this steady state is

$$\bar{\mathbf{n}} = -\mathbf{A}^{-1}\,\mathbf{p}, \tag{11}$$

which can be converted into mixing ratios by multiplying $\mathbf{n}$ by the $2N$ diagonal matrix $\mathbf{M}$ with the following elements:

$$M_{ij} = \begin{cases} \delta_{ij}/N(z_i) & i,j = 1,\cdots,N \\ \delta_{ij}/N(z_{i-n}) & i,j = N+1,\cdots,2N. \end{cases} \tag{12}$$

The time development of perturbations about this mean state is determined by the free solution in (10). Because $\mathbf{A}$ is time independent, the propagator (see equation (2)) has the form of the matrix exponential, i.e., $\mathbf{\Phi}(t) = e^{\mathbf{A}t}$.

3. Measures of Chemical Abundance

In order to proceed with the study of perturbation growth, it is necessary to adopt a measure to quantify species abundances in the initial state and a measure to quantify species abundances at a later time. These two measures need not be the same.

In many dynamical applications the appropriate measure is the euclidean or L_2 norm

$$||\mathbf{n}||_2 = \left\{\sum_{i=1}^{N} \Delta z \left[\mathbf{n}^2_{CH_3Br}(z_i) + \mathbf{n}^2_{Br_y}(z_i)\right]\right\}^{1/2}, \tag{13}$$

which is a rms measure: for chemical systems it is the euclidean length of the vector of species abundances at grid levels. Stability theory for nonnormal dynamical systems in the L_2 norm is well developed [cf. *Farrell and Ioannou*, 1996a,b].

However, the L_2 norm is not well suited for addressing questions arising in chemistry. For chemistry problems, physically appropriate perturbation measures are usually linear in the number density or mixing ratios of the constituents. One such measure is what we will call the integral measure:

$$\Delta z \left|\sum_{i=1}^{N} w_{1i}\,\mathbf{n}_{CH_3Br}(z_i) + w_{2i}\,\mathbf{n}_{Br_y}(z_i)\right|, \tag{14}$$

with $\mathbf{w}$ as a weighting factor. This measure is a weighted column abundance of the species. The weights can be chosen so that the abundances of chosen species at chosen locations contribute to the measure. An example application of (14) is to the measurement of perturbations in Br_y mixing ratio at specified locations in the stratosphere which may be of interest for assessing ozone depletion potential. For this example, w_{1i} are taken as zero and w_{2i} are taken as nonzero only at the levels of interest for the assessment. Note that the integral measure is not a norm, because there exist nonzero perturbations for which the integral measure is zero. (A vector norm is a function f from R^n to R that satisfies the following requirements: $f(x) \geq 0$ and $f(x) = 0$ if and only if $x = 0$, $f(x+y) \leq f(x) + f(y)$, and $f(\alpha x) = |\alpha| f(x)$ for all vectors x, y, and all scalars α.)

It is convenient to introduce a weighting matrix $\mathbf{W}$ to define the most general linear integral measure of chemical perturbations:

$$\left[\mathbf{n}\right]_{\mathbf{W}} \equiv \Delta z \left|\sum_{i=1}^{N_s}\sum_{j=1}^{N_s} W_{ij}\,\mathbf{n}_i\right|, \tag{15}$$

where $\mathbf{W}$ is the species measurement weighting matrix and N_s is the total dimension of the system (in the example above $N_s = 2N$ and $\mathbf{W}$ is diagonal with elements along the diagonal equal to the $\mathbf{w}$ values in (14)). When all species abundances contribute equally to the measure, $\mathbf{W} = \mathbf{I}$ (where $\mathbf{I}$ is the identity) and the integral measure will be denoted $[\mathbf{n}]$, without reference to the weighting matrix. (Note that the identity integral measure of the vector $\mathbf{Wn}$ is equal to the $\mathbf{W}$ integral measure of $\mathbf{n}$, i.e., $[\mathbf{Wn}] = [\mathbf{n}]_{\mathbf{W}}$. As a result, only the identity integral measure is needed: when a state $\mathbf{n}$

is to be measured with weighting matrix $\mathbf{W}$, it suffices to calculate the identity integral measure of $\mathbf{Wn}$.)

The linear measure with weighting matrix $\mathbf{W}$ is used to quantify abundances at a time t after the introduction of the initial perturbation. While the final state is measured with the integral measure, which need not be a norm, it is not sensible to measure the initial state in the same manner. The reason is that the integral measure can assign zero measure to nonzero perturbations, because initial perturbations of both signs can be introduced which have zero integral measure. It is necessary to measure the initial perturbations with a norm, i.e., with a measure that will give positive magnitude to all nonzero perturbations. We will employ a norm consisting of a weighted sum of the absolute values of mixing ratios (or number densities depending on context) defined as

$$||\mathbf{n}||_1^{\mathbf{W}} = \Delta z \sum_{i=1}^{N_s} \sum_{j=1}^{N_s} \left| W_{ij}\, \mathbf{n}_i \right| , \qquad (16)$$

which is the L_1 norm of the weighted vector $\mathbf{Wn}$. (The L_1 norm of a vector is equal to the sum of the absolute value of its entries, i.e., $||\mathbf{n}||_1 = \sum_i |\mathbf{n}_i|$.)

It is common in chemistry problems for the solution fields to be of one sign for initial perturbations of one sign (which requires that the propagator matrix $\mathbf{\Phi}(t)$ have all its elements of one sign). In these cases the integral measure given in (15) is equivalent to the L_1 norm, as negative perturbations can not arise if not introduced initially, so that the absolute value is redundant in (15). For example, the CH_3Br/Br_y system has a propagator with all positive elements for which the L_1 norm is appropriate.

4. Determining Optimal Growth

Having fixed the measures with which to quantify chemical perturbations, we consider the initial perturbation that produces the greatest net change at time t (the proofs and details of the methods can be found in appendix A). The ratio of the abundances at time t to the initial abundance will be called the growth at time t. The maximization problem we consider is to determine the initial state $\mathbf{n}(0)$ of unit norm, i.e., $||\mathbf{n}(0)||_1 = 1$, producing the state of maximum norm at time t, i.e.,

$$\max_{||\mathbf{n}(0)||_1=1} \left[\mathbf{n}(t)\right]_{\mathbf{W}^f} = \max_{||\mathbf{n}(0)||_1=1} \left[\mathbf{W}^f \mathbf{\Phi}(t)\mathbf{n}(0)\right] \equiv ||\mathbf{W}^f \mathbf{\Phi}(t)|| , \qquad (17)$$

where $\mathbf{W}^f$ is a measuring weighting matrix of the final state (FSW). The optimal growth in this case is denoted $||\mathbf{W}^f \mathbf{\Phi}(t)||$ in order to indicate that it depends on the propagator at the optimization time t and on the final weighting matrix $\mathbf{W}^f$.

We may want to treat a more general optimization problem in which there is weighting imposed also on the initial states in order, for example, to emphasize certain chemical constituents more than others, or to emphasize initial perturbations in selected regions. This can be done by formulating the maximization problem of determining the initial perturbation $\mathbf{n}(0)$ of unit norm that maximizes $[\mathbf{W}^f \mathbf{\Phi}(\mathbf{t})\mathbf{W}^i\mathbf{n}(0)]$, where $\mathbf{W}^i$ is a weighting matrix of the initial state (ISW). By this means we consider all initial perturbations and transfer the biases in their relative importance to the weighting matrix $\mathbf{W}^i$. For example, in the CH_3Br/Br_y system we can allow initial perturbations only in CH_3Br, in which case $\mathbf{W}^i$ is the diagonal matrix $w_{ai}\delta_{ij}$ ($a = 1, 2$), with $w_{1i} = 1$, $i = 1, \cdots N$, and $w_{2i} = 0$ for all i.

The initial perturbation producing the maximum perturbation at time t, called the optimization time, is called the optimal perturbation, and the associated maximum response resulting at time t is called the evolved optimal, and its measure is called the optimal growth. The optimal growth at time t is defined as

$$||\mathbf{W}^f \mathbf{\Phi}(t)\mathbf{W}^i|| = \max_{||\mathbf{n}(0)||_1=1} \left[\mathbf{W}^f \mathbf{\Phi}(t)\mathbf{W}^i\mathbf{n}(0)\right], \qquad (18)$$

where the notation $\max_{||\mathbf{n}(0)||_1=1}$ denotes maximization over initial perturbations $\mathbf{n}(0)$ of unit norm and the optimal growth is denoted as $||\mathbf{W}^f\ \mathbf{\Phi}(t)\ \mathbf{W}^i||$ to indicate that it depends on the propagator at the optimization time t and on the final and initial state weighting matrices $\mathbf{W}^f$ and $\mathbf{W}^i$.

Remarkably, the optimal perturbation so defined consists of excitation of a single species at the level corresponding to the column of greatest absolute sum of $\mathbf{W}^f\ \mathbf{\Phi}(t)\ \mathbf{W}^i$, and the optimal growth is this sum (appendix A). In the continuous limit the optimal perturbation approaches a delta function of a single species at a specific level. This delta function subsequently evolves with time as the Green's function of the operator. A similar result is obtained if the final state is measured in the L_1 norm, except in this case the optimal perturbation consists of excitation of a single species at the level corresponding to the column of $\mathbf{W}^f\ \mathbf{\Phi}(t)\ \mathbf{W}^i$ with the greatest sum of the absolute values of its elements, and the optimal growth is this sum.

The same magnitude of perturbation growth is obtained for the positive and the negative delta functions: in the first case we have identified the perturbation with growth of greatest positive measure, while in the second case we have identified the perturbation with growth of greatest negative measure. In general, the initial perturbation producing the final perturbation of minimum magnitude in the integral measure is not a spatial delta function of a single species. However, the minimum growth in magnitude in the L_1 norm is a delta function of a single species at the single location corresponding to the column of $\mathbf{W}^f\ \mathbf{\Phi}(t)\ \mathbf{W}^i$ with minimum sum of the absolute value of its elements. We can exploit this simple result when minimum impact is sought in the integral measure even in cases when positivity of the unrestricted propagator is not assured, because it is of-

ten possible to choose an appropriate FSW to ensure positivity and allow the minimum to be identified with a delta function initial perturbation as the integral measure then becomes the L_1 norm.

It is a remarkable property that if the propagator is known, then we can determine the optimal perturbation in the integral measure by determining the column of the propagator with the maximum absolute sum. While for small-dimensional examples, obtaining the propagator with matrix manipulations is certainly possible, this is impossible in large global chemical models. The propagator could be obtained in that case by integrating forward the identity matrix, which requires a number of integrations equal to the dimensionality of the system. However, this is a numerically expensive procedure. In meteorology where L_2 optimal perturbations are obtained routinely in the course of operational forecasting, this problem is solved by singular value decomposition using iterative techniques based on forward time integration of the model, followed by backward integration of the adjoint model until a subset of optimals and evolved optimals has been found. Because of the linearity of the measure in chemical models, a great simplification occurs, and chemical optimal perturbations can be determined by a single integration of the transposed dynamical system.

This result follows immediately from the observation that the transposed dynamical system, with dynamical operator $\mathbf{A}^T$, has as its propagator $\mathbf{\Phi}(t)^T$, as $(e^{\mathbf{A}t})^T = e^{\mathbf{A}^T t}$. Consider the initial condition $\mathbf{n}(0) = [1, 1, \cdots, 1]^T$. This initial condition will evolve to

$$\tilde{\mathbf{n}}(t) = \mathbf{\Phi}(t)^T \mathbf{n}(0) \,, \tag{19}$$

which is a vector with entries the sums of the columns of $\mathbf{\Phi}(t)$. The entry of $\tilde{\mathbf{n}}(t)$ with the maximum value determines the optimal growth at time t. If this maximum value occurs at the kth entry of $\tilde{\mathbf{n}}(t)$, then the optimal perturbation is the unit vector $\mathbf{n}_{\text{opt}}$, with entries $(\mathbf{n}_{\text{opt}})_i = \delta_{ik}$. The evolved optimal is then obtained by forward integration to time t of the system with initial condition $\mathbf{n}_{\text{opt}}$. Therefore, without obtaining the propagator we can determine the optimal perturbation with a single adjoint integration and the evolved optimal with one more integration of the system.

If, now, we want to determine the perturbation that leads to the optimal growth $||\mathbf{W}^f \, \mathbf{\Phi}(t) \, \mathbf{W}^i||$, we consider the initial condition

$$\mathbf{n}(0) = (\mathbf{W}^f)^T \, [1, 1, \cdots, 1]^T \,, \tag{20}$$

which we integrate forward by the transpose system $\mathbf{A}^T$ to obtain

$$\tilde{\mathbf{n}}(t) = \mathbf{\Phi}(t)^T \mathbf{n}(0) \,. \tag{21}$$

The maximum entry of $(\mathbf{W}^i)^T \tilde{\mathbf{n}}(t)$ is the optimal growth. If the maximum occurs at the kth entry of $(\mathbf{W}^i)^T \tilde{\mathbf{n}}(t)$, then the optimal perturbation is the unit vector $\mathbf{n}_{\text{opt}}$, with entries $(\mathbf{n}_{\text{opt}})_i = \delta_{ik}$. The evolved optimal is then obtained by forward integration to time t of the system with initial condition $\mathbf{n}_{\text{opt}}$.

In the asymptotic limit $t \to \infty$, all initial perturbations assume the structure of the least damped mode and decay at a rate given by the real part of the least damped mode eigenvalue. This suggests the problem of determining the initial perturbation which optimally excites the least damped mode and consequently produces the greatest disturbance to the system as $t \to \infty$. In the integral measure it turns out that the initial perturbation that optimally excites the least damped mode is a delta function of a single species located at the level corresponding to the maximum amplitude not of the mode itself but of its quite distinct bi-orthogonal (see section 1). The proof of this theorem is given in appendix B. The structure of the bi-orthogonal differs from that of the mode in nonnormal systems. The bi-orthogonal can be obtained either by inverting the matrix of the eigenvectors or by eigenanalysis of the transpose operator $\mathbf{A}^T$.

Often it is required to maximize the integrated concentration of a species at a chosen location after a pulsed emission. For example, the ozone depletion potential is given by the time integral of Br_y concentration in the stratosphere [*Prather*, 1996, 1997]. It is thus required to obtain

$$||\mathbf{W}^f \left(\int_0^\infty e^{\mathbf{A}t} dt \right) \mathbf{W}^i|| = || - \mathbf{W}^f \mathbf{A}^{-1} \mathbf{W}^i||, \tag{22}$$

for some initial weighting $\mathbf{W}^i$ and final weighting $\mathbf{W}^f$. The solution to this problem is to locate the pulse at a level corresponding to the column of $\mathbf{W}^f \, \mathbf{A}^{-1} \, \mathbf{W}^i$ with the maximum absolute sum.

5. Example

As an example, consider the $\text{CH}_3\text{Br}/\text{Br}_y$ system. The eigenmodes of this system can be separated into two classes: modes that involve only Br_y perturbations (the Br modes) and those that involve both CH_3Br and Br_y perturbations (the CH_3Br modes) [*Prather*, 1997]. The least damped CH_3Br mode with only diffusion (no advection) is shown as curve 1 in Figure 2; it has a decay time of 2.1 years. Its bi-orthogonal (for calculation of the bi-orthogonal see section 1) consists of only CH_3Br perturbation and is also shown in Figure 2 (curve 2). Optimal excitation in the integral measure of this least damped CH_3Br mode is obtained by placing a CH_3Br perturbation in number density at 19.4 km, where the bi-orthogonal reaches its maximum, which results in approximately a twofold increase in amplitude of the mode over introduction of the mode itself as an initial perturbation. Advection reduces the decay times and shifts the maximum amplitude of the mode to higher altitudes while its bi-orthogonal is shifted toward the ground as can be shown in Figure 3 for the case of maximum advection $w = 300$ m d^{-1} in the midtroposphere and $w = 30$ m d^{-1} in the stratosphere (see Figure 1b).

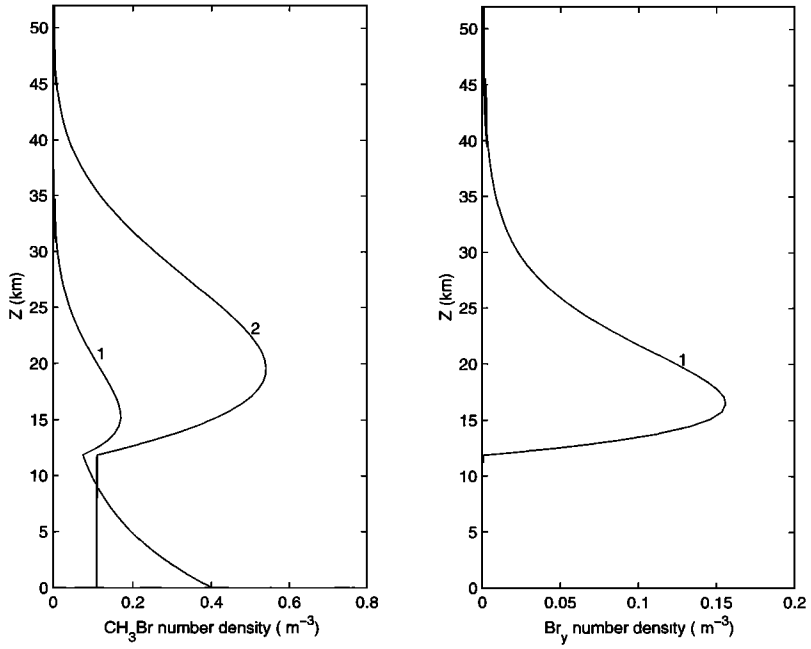

Figure 2. (left) CH_3Br number density. (right) Br_y number density. Curve 1 shows the vertical structure of the least damped CH_3Br mode for zero advection (decay time 2.1 years). Curve 2 shows the bi-orthogonal of this mode which comprises only a CH_3Br perturbation. Optimal excitation of the mode in the integral measure is achieved by placing unit CH_3Br perturbation at 19.4 km where the bi-orthogonal has its maximum. The modes have been normalized to unity in L_2.

For this case the least damped CH_3Br mode (curve 1) has a decay time of 1.48 year. Its bi-orthogonal (curve 2) is again a perturbation in CH_3Br alone. The optimal excitation is impulsive introduction of CH_3Br at the ground, which leads to a factor 1.6 increase in the amplitude of the mode compared with the amplitude that would have been obtained if the mode itself were introduced initially. Examination of the structure of the bi-orthogonals in Figures 2 and 3 reveals that the least damped mode can be effectively excited by CH_3Br perturbations in the stratosphere in the example with diffusion only (Figure 2) while inclusion of advection in the dynamics renders CH_3Br perturbations in the stratosphere totally ineffective in exciting the least damped mode (Figure 3).

As an example of optimal excitation, we consider the problem of finding the initial perturbations with the greatest ozone depletion potential which requires a FSW that identifies the mixing ratio concentrations of Br_y in the lower stratosphere. For that purpose a suitable final state weighting is $\mathbf{W}^f = \mathbf{P}\,\mathbf{M}$, where $\mathbf{M}$ is the matrix (equation (12)) that converts number densities into mixing ratios and $\mathbf{P}$ projects the final state to the Br_y species at 20 km; that is, $P_{kl} = \delta_{l\alpha}\delta_{kl}$ (no summation), where α is the index of Br_y at the level of 20 km. We allow initial number density perturbations only in CH_3Br, so the initial state weighting is $W^i_{kl} = \delta_{kl}$ for the CH_3Br entries $(k, l \leq N)$ and zero otherwise. We normalize the initial CH_3Br to correspond to the number density that would result in a mixing ratio of 1 parts per trillion (ppt) over the first 2 km above the ground. The optimal growth at time t is given by the integral measure of the propagator $||\mathbf{W}^f e^{\mathbf{A}t}\mathbf{W}^i||$ (see equation (18)), which because of positivity of the propagator is the same as its L_1 norm which equals the greatest absolute column sum of the matrix $\mathbf{W}^f e^{\mathbf{A}t}\mathbf{W}^i$.

The optimal mixing ratio of Br_y at 20 km and the location of the initial CH_3Br perturbation as a function of time are shown in Figure 4 for the case in which both advection and diffusion are present. The evolution of two optimal initial conditions is also shown: the optimal for 6 years and the optimal for 2 months. For large times (in this model for $t > 5.5$ years), optimal mixing ratios of Br_y are obtained by placing the CH_3Br perturbation at the ground. For intermediate times it is best to place the CH_3Br perturbation at the top of the stratosphere, while for the shortest times the optimal is near the target level. The level of injection that would result in the least CH_3Br response is also shown in figure 4. The maximum possible growth is called the global optimal, and it occurs at a time which will be referred to as a global optimal time. For the chosen parameters this is 1 year. Consequently, at least for a year following the introduction of a perturbation, decay time estimates based on the inverse of the decay rate of the least damped mode are not valid. In fact, for the chosen parameters the least damped mode decay rate (decay time of 1.48 years) is not obtained until 4 years after an impulsive excitation.

The global optimal time decreases with increasing ad-

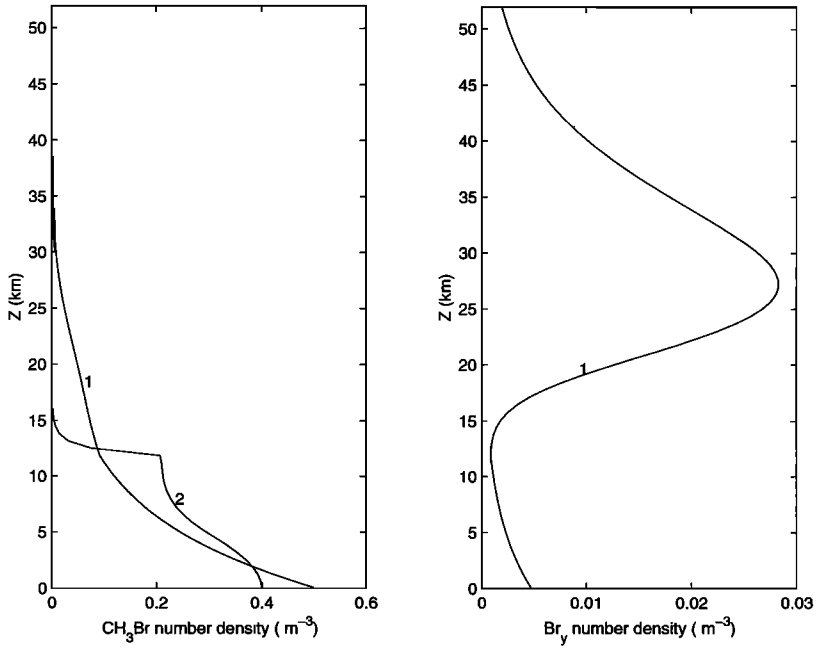

Figure 3. (left) CH_3Br number density. (right) Br_y number density. Curve 1 shows the vertical structure of the least damped CH_3Br mode with advection. The decay time of the mode is 1.48 years. Curve 2 shows the bi-orthogonal of this mode which comprises only a CH_3Br perturbation. Optimal excitation of the mode in the integral measure is achieved by placing unit CH_3Br perturbation at the ground where the bi-orthogonal has its maximum. The modes have been normalized to unity in L_2.

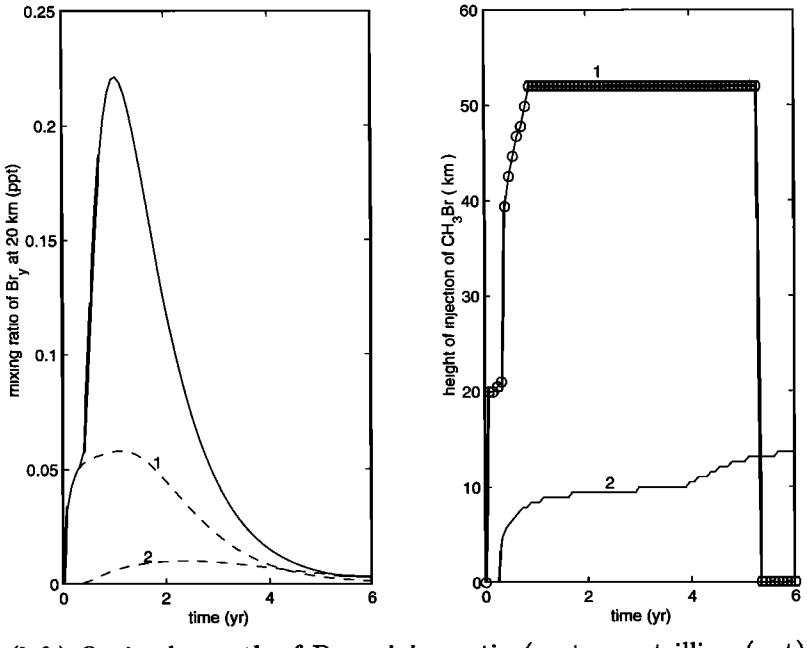

Figure 4. (left) Optimal growth of Br_y mixing ratio (parts per trillion (ppt)) at 20 km as a function of optimization time. Optimization time is defined as the time selected to calculate the maximum possible growth (the optimal growth) in the system as quantified by the selected measure of chemical perturbations, which is here the mixing ratio of Br_y at 20 km. Only CH_3Br initial perturbations are considered. The amount released at the ground over a grid interval Δz is equivalent to 1 ppt over the first 2 km (4.8×10^{16} m^{-2}). Both advection and diffusion are included. Dashed curve 1 shows the time evolution of the 2 month optimal perturbation. Dashed curve 2 shows the time evolution of the 6 year optimal perturbation, which is initially at the ground. (right) Height (kilometers) of the optimal CH_3Br perturbation is shown as a function of optimization time (curve 1). Height (kilometers) of the initial perturbation in CH_3Br that leads to the least response in Br_y mixing ratio at 20 km is shown as a function of optimization time (curve 2).

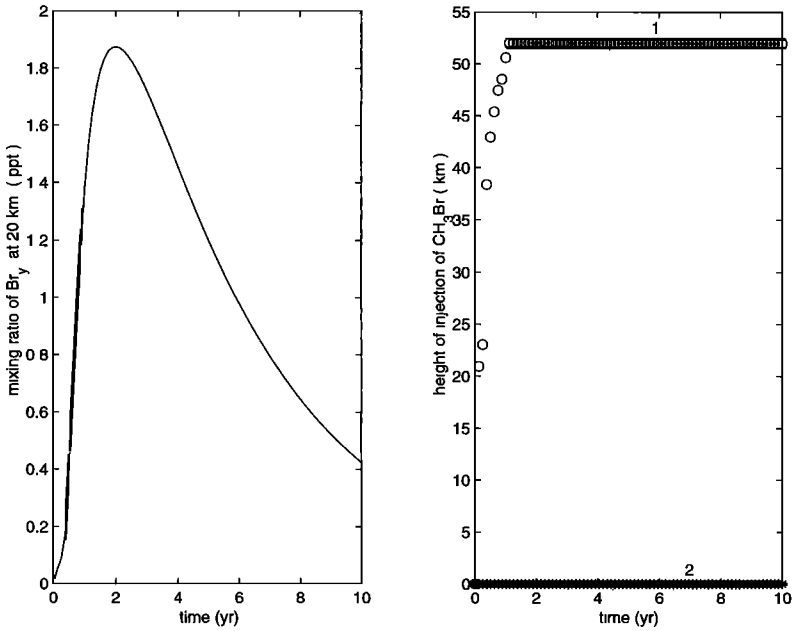

Figure 5. (left) Optimal growth of Br_y mixing ratio (ppt) at 20 km as a function of optimization time. Optimization time is defined as the time selected to calculate the maximum possible growth (the optimal growth) in the system as quantified by the selected measure of chemical perturbations which is here the mixing ratio of Br_y at 20 km. Only CH_3Br initial perturbations are considered. The amount released at the ground over a grid interval Δz is equivalent to 1 ppt over the first 2 km (4.8×10^{16} m^{-2}). Only diffusion is included (no advection). (right) Height (kilometers) of the optimal CH_3Br perturbation is shown as a function of optimization time (curve 1). Height (kilometers) of the initial perturbation in CH_3Br that leads to the least response in Br_y mixing ratio at 20 km is shown as a function of optimization time (curve 2).

vection, while the qualitative features of the optimal excitation remain. The optimal growth and levels of optimal excitation for different optimizing times with no advection are shown in Figure 5. The optimal level for CH_3Br perturbations is always aloft, while perturbations at the ground produce the minimal response. The global optimal time is about 2 years and the asymptotic decay time of 2.1 years is obtained after 5 years. Again, estimates of species lifetime based on the asymptotic decay of the least damped mode of the system are valid only after the transient buildup phase has ended, which in our example requires 4 years.

6. Lifetimes

Traditional methods for analyzing response of chemical equilibria to perturbation proceed from the concept of a representative lifetime. If a chemical equilibrium concentration $n(t)$ were governed by a scalar differential equation of the form

$$\frac{dn}{dt} = -\alpha n + p \ , \tag{23}$$

then an initial perturbation $n(0)$ would decay back toward the equilibrium concentration p/α as

$$n(t) = e^{-\alpha t}\, n(0) + \frac{p}{\alpha} \ , \tag{24}$$

and a decay timescale $\tau_d = 1/\alpha$ characterizing the return of the system to equilibrium is well founded. Also, the reservoir turnover time given by the steady state abundance $n(\infty) = p/\alpha$ divided by the forcing p, $\tau_r = n(\infty)/p = 1/\alpha$, is equal to τ_d and is also well founded. However, if the system is multidimensional, then there are as many such timescales as the dimension of the system, because each mode has an associated timescale given by the reciprocal of its damping rate.

To further examine the concept of a representative lifetime, we first obtain a reservoir turnover time for our nonnormal system by solving the forced equation

$$\frac{d\mathbf{n}}{dt} = \mathbf{A}\mathbf{n} + \mathbf{p}(t) \ , \tag{25}$$

for a time-varying forcing $\mathbf{p}(t)$ with mean $\bar{\mathbf{p}}$. The mean state forced response (appendix D) is

$$\bar{\mathbf{n}} = -\mathbf{A}^{-1}\,\bar{\mathbf{p}} \ . \tag{26}$$

If the forcing is confined to CH_3Br at the ground level and the amplitude of the forcing is chosen to produce 10 ppt at the ground at equilibrium, the resulting profile is as shown in Figure 6. The reservoir timescale is found by taking the ratio of the total abundance (m^{-3}) to the input rate (m^{-3} s^{-1}):

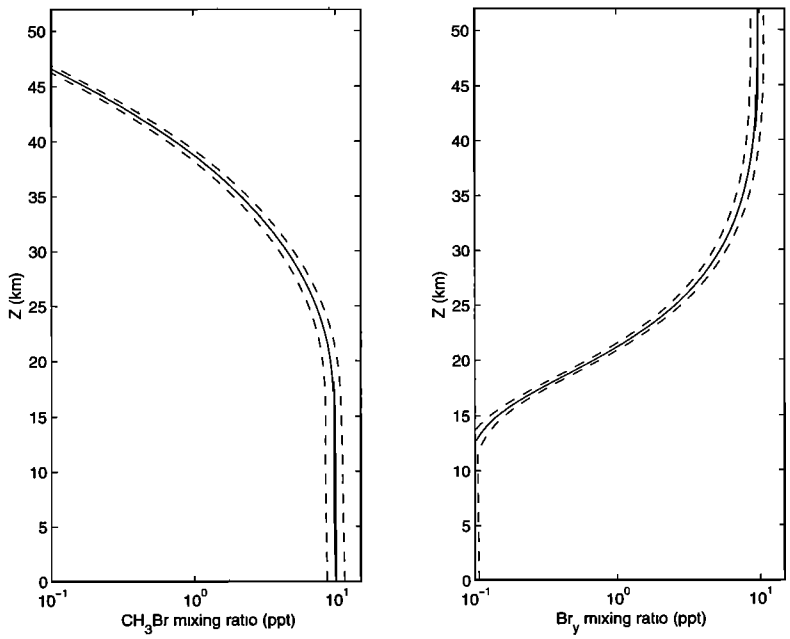

Figure 6. Mixing ratio maintained by a fluctuating source of CH_3Br at the ground. The source has a mean of 0.09 ppt d^{-1} and a variance of 1 ppt^2 $(12\ min)^{-2}$. Vertical advection is included. (left) Vertical distribution of mean CH_3Br. (right) Vertical distribution of Br_y. The dashed curves signify one standard deviation from the mean.

$$\tau_r = \frac{||\bar{\mathbf{n}}||_1}{||\bar{\mathbf{p}}||_1} \quad . \tag{27}$$

This timescale is sensitive to the location of the forcing and to the nonnormality of $\mathbf{A}$ (for an explanation, see appendix D). The result of moving the forcing is shown in Figure 7. The reservoir timescale does not accurately reflect either the decay rate of transient perturbations at short time or the asymptotic decay rate at long times.

An alternative timescale is the relaxation timescale obtained after removal of the steady forcing maintaining the equilibrium state. This produces a continual variation of decay rates, implying decay times varying as

$$\tau(t) = \left[\frac{d||e^{\mathbf{A}t}\ (\mathbf{A}^{-1}\bar{\mathbf{p}})||_1}{dt} \right]^{-1} , \tag{28}$$

finally approaching the decay time of the least damped mode. This timescale depends on time elapsed since removal of the forcing, on the location of the forcing, and on the nonnormality of the evolution operator through the condition number of $\mathbf{A}^{-1}$. An example for forcing of CH_3Br at the ground is shown in Figure 8. Relaxation from the equilibrium state of a normal system proceeds with the instantaneous decay times monotonically increasing and asymptotically approaching the decay time of the least damped mode. Examination of Figure 9 reveals that this is not the case for the evolution of either CH_3Br or Br_y in the advecting case and is true only for relaxation of CH_3Br in the purely diffusive case. This reveals that the dynamics of number density evolution of both species in the presence of advection are dominated by nonnormality while the number density evolution of CH_3Br in the diffusive case is essentially that of a normal system. The degree of nonnormality depends on the variable we choose to study. As an example, the relaxation timescales for mixing ratios in the purely diffusive case are compared in Figure 9 to the relaxation times for number density. It is clear that the timescales depend on the choice of variable and also that the dynamics of mixing ratios have a greater degree of nonnormality than do the dynamics of number densities. The relaxation of CH_3Br is determined by a highly nonnormal operator when the variable is mixing ratio while when the variable is number density the governing operator is essentially normal. As a result, the decay times for mixing ratio are initially greatly increased compared with the decay times for number density. However, if one waits long enough for the asymptotic regime to be obtained, then the relaxation timescale becomes the decay time of the least damped mode which is sometimes thought to be the sole fundamental timescale of the system.

A third timescale is obtained from observing the size of fluctuations in the system. The fluctuation variance maintained by forcing CH_3Br stochastically at the ground is shown in Figure 6 (appendix C). In analogy with a scalar equation,

$$\frac{dn}{dt} = -\alpha n + \gamma \epsilon_t \ , \tag{29}$$

with ϵ_t as a white noise forcing with zero mean and unit variance. The maintained variance is

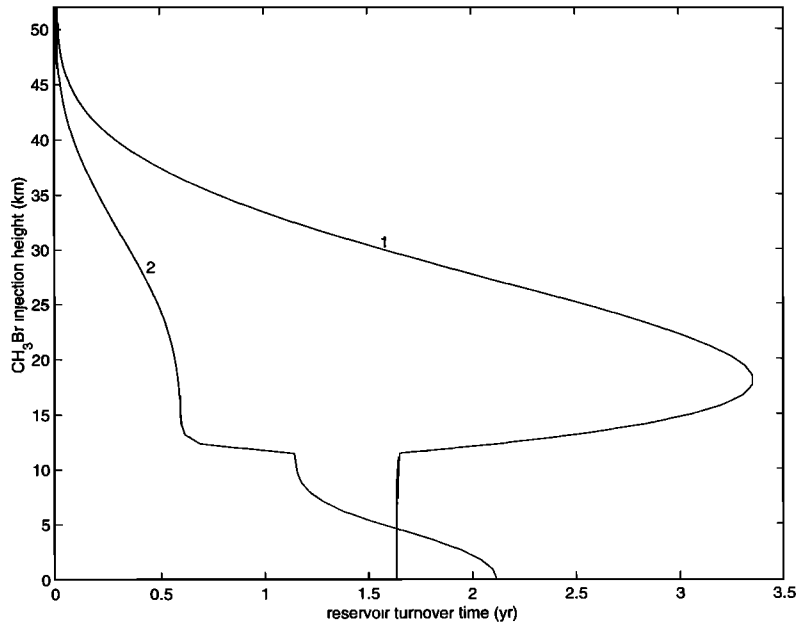

Figure 7. Reservoir turnover time as a function of the CH_3Br source height. Curve 1 shows turnover times with only diffusion included. Curve 2 shows turnover times with both advection and diffusion included.

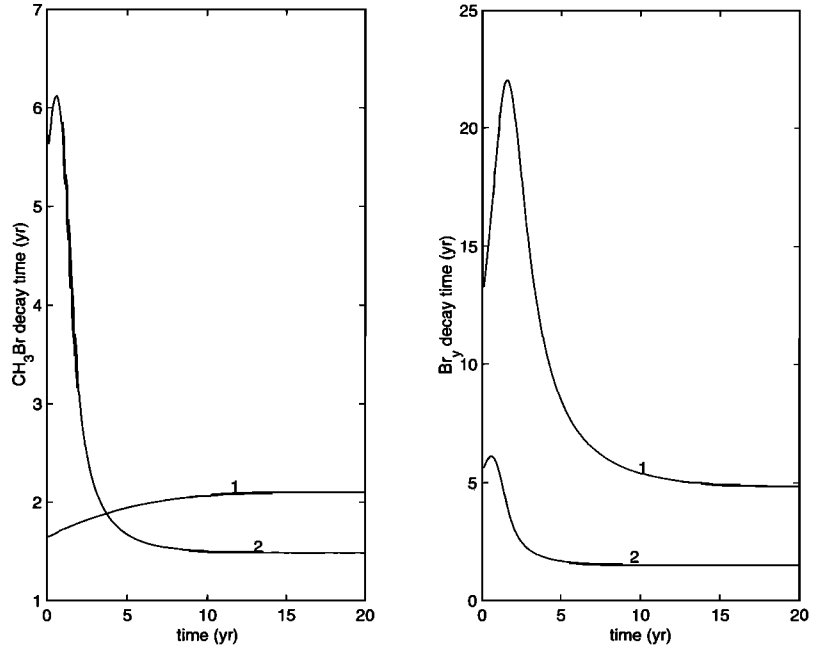

Figure 8. Timescales for relaxation from the equilibrium produced by a constant CH_3Br source at the ground. (left) Instantaneous decay rate of CH_3Br expressed as a timescale as a function of time from removal of the source. Curve 1 shows relaxation timescales with only diffusion included. Curve 2 shows relaxation timescales with both advection and diffusion included. (right) Instantaneous decay rate of Br_y expressed as a timescale as a function of time from removal of the source. Curve 1 shows instantaneous decay rates with only diffusion included. Curve 2 shows instantaneous decay rates with both advection and diffusion included. In all cases the decay time approaches that of the least damped mode for large t, but for an interval of time of approximately 5 years after removal of the source, the decay time differs substantially from that of the least damped mode.

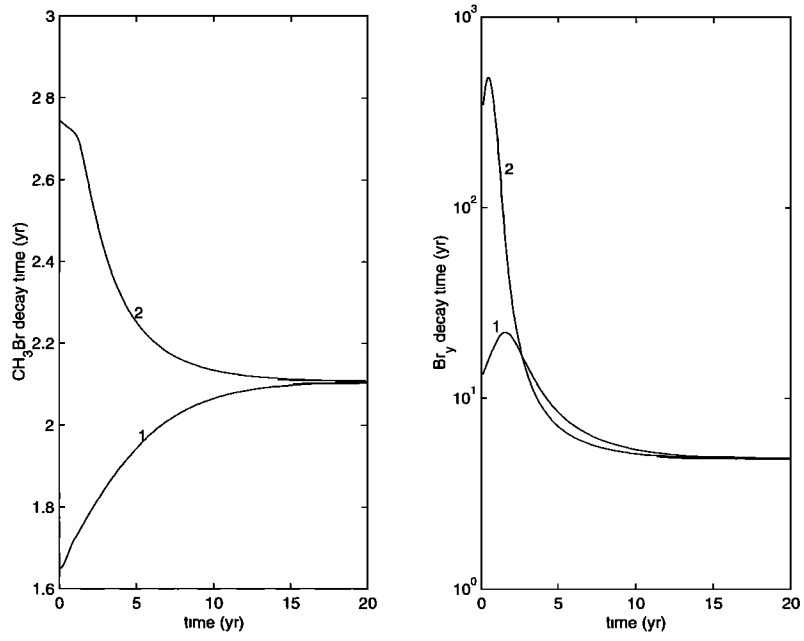

Figure 9. Relaxation timescales from an equilibrium state produced by a constant CH_3Br source at the ground for the case of no advection. The influence of variable choice is revealed by the contrast between two cases. Curve 1 shows the instantaneous decay time of number density as a function of time from removal of the source. (left) CH_3Br. (right) Br_y. Curve 2 shows the instantaneous decay time of mixing ratio as a function of time from removal of the source.

$$< n^2 > \; = \; \frac{\gamma^2}{2\alpha}, \tag{30}$$

from which the timescale

$$\tau_f \; = \; \frac{2 < n^2 >}{\gamma^2} \tag{31}$$

can be estimated. For our example the mean mixing ratio variance in the troposphere together with the forcing at the ground yield from (31) a timescale of 25 days. This estimated timescale is short because white noise forcing projects substantially on modes which are damped more rapidly than the modes primarily excited by the zero-frequency mean forcing. This frequency dependence of the timescale can be examined further by Fourier analysis of the perturbation version of (25):

$$\frac{d\mathbf{n}'}{dt} \; = \; \mathbf{A}\mathbf{n}' \; + \; \mathbf{p}'(t), \tag{32}$$

where $\mathbf{p}'(t) = \mathbf{p}(t) - \bar{\mathbf{p}}$; with transformed variable

$$\hat{\mathbf{n}}(\omega) = \frac{1}{2\pi} \int_{-\infty}^{\infty} \mathbf{n}'(t) e^{-i\omega t} dt \, , \tag{33}$$

the response at frequency ω for the transformed forcings,

$$\hat{\mathbf{p}}(\omega) = \frac{1}{2\pi} \int_{-\infty}^{\infty} \mathbf{p}'(t) e^{-i\omega t} dt \, , \tag{34}$$

weighted by $\mathbf{W}^i$ can be expressed as

$$\hat{\mathbf{n}}(\omega) \; = \; \mathbf{R}(\omega) \; \mathbf{W}^i \; \hat{\mathbf{p}}(\omega) \, , \tag{35}$$

in terms of the resolvent:

$$\mathbf{R} \; = \; (i\omega \mathbf{I} - \mathbf{A})^{-1} \, , \tag{36}$$

where $\mathbf{I}$ is the identity. In analogy with (21) we can define a damping time as a function of frequency to be the ratio of the total abundance (m^{-3}) to the input rate (m^{-3} s^{-1}). For sinusoidal forcing at frequency ω this timescale is

$$\tau_\omega \; = \; \frac{|| \; \hat{\mathbf{n}}(\omega) \; ||_1}{|| \; \mathbf{W}^i \hat{\mathbf{p}}(\omega) \; ||_1} \; . \tag{37}$$

At zero frequency this damping time is identical to the reservoir turnover time, but the damping time dramatically decreases with increasing frequency as shown in Figure 10. Consequently, timescales based on reservoir turnover time overestimate the persistence of perturbations associated with small temporal scale which have high frequency components in their Fourier representation.

When all frequencies are excited equally as would be the case for uncorrelated white noise forcing of unit variance, i.e., $< \hat{p}_i(\omega_1) \; \hat{p}_j^*(\omega_2) > \; = \; \delta_{ij} \; \delta(\omega_1 - \omega_2)/2\pi$, the mean ensemble response variance weighted by $\mathbf{W}^f$, $\tilde{\mathbf{n}} = \mathbf{W}^f \mathbf{n}$, is

$$< |\tilde{\mathbf{n}}|^2 >= \frac{1}{2\pi} \int_{-\infty}^{\infty} F(\omega) \, d\omega, \tag{38}$$

in which the power spectrum is given by

$$F(\omega) = \text{trace} \; (\mathbf{W}^f \; \mathbf{R} \; \mathbf{W}^i \; \mathbf{W}^{iT} \; \mathbf{R}^\dagger \; \mathbf{W}^{fT}) \, , \tag{39}$$

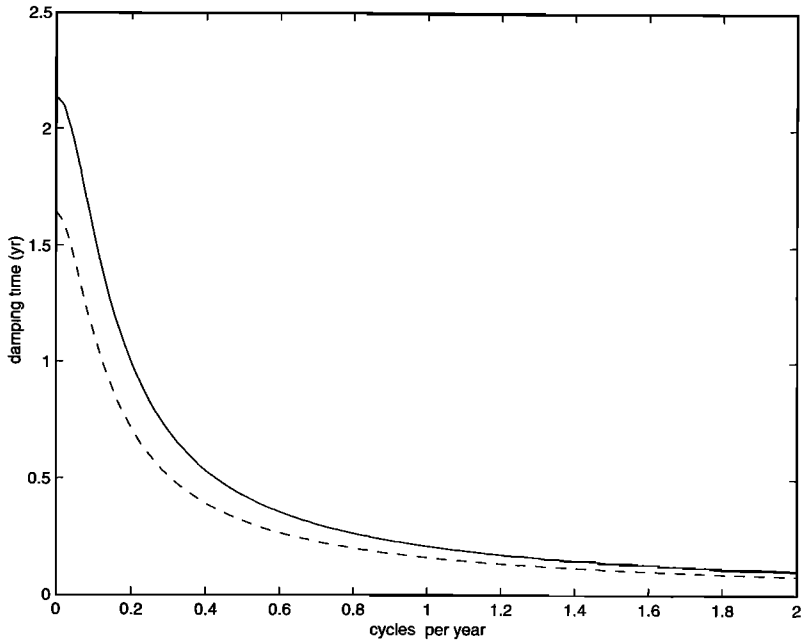

Figure 10. The damping time of troposphere-averaged CH_3Br number density (years) as a function of the frequency of the forcing of CH_3Br at the ground (cycles per year). Dashed curve shows damping time with only diffusion included. Continuous curve shows damping time with both advection and diffusion included.

where † denotes the hermitian transpose and $< |\tilde{\mathbf{n}}|^2 >$ denotes the stationary ensemble variance. For forcing at the ground the power spectrum of mean CH_3Br mixing ratio variance over the troposphere ($0 - 10$ km) is shown in Figure 11 for forcing fluctuations with standard deviation 1 ppt per 12 min, as was used in the example shown in Figure 6.

7. Conclusions

A central problem in chemical dynamics is to determine the response of chemical equilibria to perturbation. This problem arises, for instance, in connection with assessing the impact of natural or anthropogenic sources. Traditional methods for addressing this problem include estimation of lifetimes from reservoir turnover times at equilibrium and calculation of modal decay rates. However, these methods may not be adequate to comprehensively analyze the response of chemical equilibria to perturbation particularly in cases in which these systems are nonnormal. Properties of the solutions of nonnormal systems are most effectively revealed by analysis of the system propagator. Methods based on the system propagator generalize directly to time-dependent problems while methods based on eigenanalysis do not generalize, because eigenmodes are not defined for time-varying systems. Among the general properties obtained using the methods of nonnormal system analysis which were illustrated using a model system in this work are bounds on optimal growth in the L_1 norm (sum of the absolute values of concentrations) and integral measure (absolute value of the sum of concentrations), the resulting growth as a function of time, the perturbation producing the optimal growth, the time period after which asymptotic decay rates are obtained, the response of the system to stochastic forcing applied impulsively and continually, and measures of timescales.

Because the perturbation chemical equilibrium system is linear and the appropriate measures are also linear, the optimal perturbation is a delta function corresponding to the introduction of a disturbance in the concentration of a single species at a single spatial location. At least conceptually, this greatly simplifies the problem of determining the optimal, because only a number of points equal to the dimension of the system are candidate optimals, while to determine the optimal in the L_2 norm, which is nonzero at all levels, it is necessary to search all vectors $\mathbf{n}$ in R^N satisfying $||\mathbf{n}||_2 = 1$, where N is the dimension of the system, which is a far wider space of candidate optimals. Remarkably, in the linear measures appropriate for chemistry a far greater simplification is possible: the optimal can be determined by inspection of the components of a single vector obtained from integration of the transposed system matrix.

The optimal excitation of a mode was found to be a delta function at the location corresponding to the maximum absolute value of the bi-orthogonal of the mode rather than of the mode itself. If the mode excited is

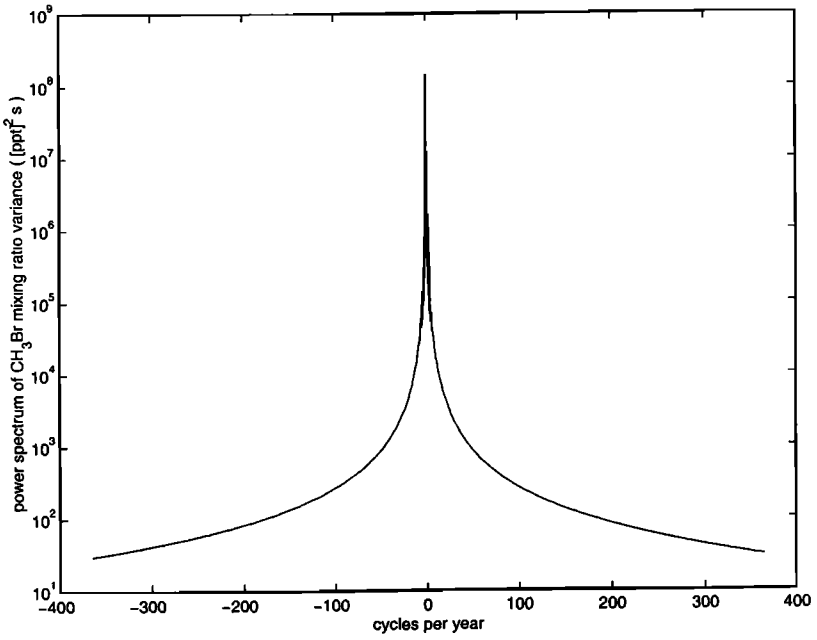

Figure 11. Power spectrum of CH_3Br mixing ratio variance averaged over the troposphere (0 – 10 km) resulting from white noise forcing of CH_3Br at the ground. The frequencies shown correspond to periods longer than a day. The peak response occurs for stationary forcing, and the response falls off rapidly with increasing frequency. Vertical advection is included.

the least damped mode, this corresponds to excitation of the most persistent perturbation. The excitation of the mode by placing a delta function initial concentration at the location where the absolute value of the biorthogonal is maximum leads to excitation of the mode at an amplitude which may far exceed the magnitude that would have been obtained if the mode itself were introduced initially (in the simple CH_3/Br_y example this led to a twofold increase of the amplitude of the least damped mode).

A single timescale for perturbations to a chemical equilibrium system with more than one degree of freedom does not exist, and only in the case that a single mode is excited is a single timescale obtained, and the timescale associated with the decay rate of the least damped mode is appropriate only in the asymptotic limit, assuming that a spectrum of modes is excited. Timescales based on reservoir turnover times and on relaxation from equilibrium depend on the spatial distribution of the species at equilibrium and the nonnormality of the system matrix. Moreover, reservoir timescales and timescales based on relaxation from equilibrium depend on the nonnormality of the operator, which in turn depends on the variable chosen and the measure used. Timescales obtained from observations of fluctuation variance require knowledge of the spatial distribution of the forcing and are, in general, short compared to the reservoir and relaxation from equilibrium timescales due to the excitation of highly damped high-frequency perturbations.

Appendix A: Optimal Growth and Optimal Perturbations in the Integral Measure

Consider the $N \times N$ propagator matrix $\mathbf{\Phi}(t)$ and a vector of number densities $\mathbf{n} = \sum_{i=1}^{N} \gamma_i \, \mathbf{e}^i$, where $\mathbf{e}^i$ is the canonical basis column vector with elements $e^i_j = \delta_{ij}$, and $\sum_{i=1}^{n} |\gamma_i| = 1$ so that $||\mathbf{n}||_1 = 1$. We have

$$\begin{aligned} \left[\mathbf{\Phi}(t)\mathbf{n}\right] &= \left| \sum_{i=1}^{N} \sum_{j=1}^{N} \gamma_j \, \Phi_{ij}(t) \right| \\ &\leq \sum_{j=1}^{N} |\gamma_j| \left| \sum_{i=1}^{N} \Phi_{ij}(t) \right| \\ &\leq \max_j \left[\left| \sum_{i=1}^{N} \Phi_{ij}(t) \right| \right], \end{aligned} \tag{A1}$$

where the last inequality follows from the fact that each $|\gamma_i| \leq 1$ and the maximum sum over j corresponds to the column of $\mathbf{\Phi}(t)$ with maximum absolute sum. The maximum value of $\left[\mathbf{\Phi}(t)\mathbf{n}\right]$ over all unit vectors $\mathbf{n}$ is attained for the canonical basis vector $\mathbf{n} = \mathbf{e}^j$, where j is the column of $\mathbf{\Phi}(t)$ with the maximum absolute sum. We have proven that the optimal growth in the integral measure of the propagator, $||\mathbf{\Phi}(t)||$, is the largest absolute column sum of $\mathbf{\Phi}(t)$ and that the optimal vec-

tor producing this growth is the canonical basis vector corresponding to this column.

Similar results hold if instead of the integral measure, we consider the L_1 norm. The maximum value of $||\mathbf{\Phi}(t)\mathbf{n}||_1$ over vectors $\mathbf{n}$ of unit norm is attained for the canonical basis vector $\mathbf{n} = \mathbf{e}^j$, where j is the column of $\mathbf{\Phi}(t)$ with the maximum sum of the absolute values of its elements. Additionally, the perturbation producing the minimal disturbance in L_1 (although not necessarily in integral measure) is a canonical basis vector corresponding to the minimum column sum of the absolute values of the propagator.

This theorem permits a rapid search for the optimal growth and its optimal excitation. It is only required to determine the column of the propagator with maximum absolute sum. The optimal perturbation will be a unit perturbation at the corresponding level.

Although linear measures are often most appropriate for measuring chemical perturbations, in order to fix ideas it is useful first to consider the case in which the chosen perturbation measure is the L_2 norm. Then the optimal growth at time t is the norm of the weighted propagator initial perturbations of unit euclidean magnitude:

$$||\mathbf{W}^f e^{\mathbf{A}t} \mathbf{W}^i||_2 = \max_{||\mathbf{n}||_2=1} ||\mathbf{W}^f e^{\mathbf{A}t} \mathbf{W}^i \mathbf{n}||_2 \quad . \quad \text{(A2)}$$

Optimal growth at t in the L_2 norm is found by singular-value decomposition of the propagator $\mathbf{W}^f e^{\mathbf{A}t}\mathbf{W}^i$, and by this means a complete set of orthogonal perturbations is obtained, which can be ordered according to growth [*Farrell and Ioannou*, 1996a]. Analysis of transient growth in the integral measure appropriate for chemistry is less complete than that based on the L_2 norm, because this measure is not derived from an inner product, and consequently there is no associated concept of orthogonality by which to separate perturbations so that the perturbations can be ordered in contribution to the vector norm.

The results on the optimal perturbation in the integral norm can be illustrated and related to the familiar properties of the L_2 norm by considering the action on unit vectors of the model 2×2 propagator:

$$\mathbf{\Phi}(t) = \begin{pmatrix} -1 & -2 \\ 4 & 4 \end{pmatrix} \quad . \quad \text{(A3)}$$

In the L_2 norm the locus of the initial vectors of unit norm $||\mathbf{n}||_2 = 1$ is a unit circle in the (n_1, n_2) plane which is distorted into an ellipse by the action of the propagator matrix as illustrated in Figure 12. The length of the major semi-axis of this ellipse OB' gives the optimal growth, and the vector **OB** that is mapped to it is the optimal vector producing this growth. For this specific example the L_2 norm of the matrix is 6.05.

Consider now the unit vectors in the L_1 norm. The locus of initial vectors of unit norm $||\mathbf{n}||_1 = 1$ is the inscribed square which intersects the unit circle at the coordinate axes. This square is distorted into a parallelogram inscribed in the ellipse by the action of the propagator. We know from the above theorem that the optimal perturbation is located at one of the vertices of the inscribed square. A check of the vertices of the inscribed square reveals that the vertex C, which is mapped to C', is the optimal perturbation in the L_1 norm, and the optimal growth is the L_1 norm of **OC′**, which is $||\mathbf{OC}'||_1 = 6$. The maximum growth in the integral measure is also achieved at one of the vertices, and a check of the vertices of the inscribed square reveals that this optimal perturbation is A, which is mapped to A'. The optimal growth is the integral measure of **OA′**, which is $[\mathbf{OA}'] = 3$. Because the elements of the propagator $\mathbf{\Phi}$ have mixed signs the maximum absolute sum of the columns (the integral measure) differs from the sum of the absolute values of the columns (the L_1 norm). Note that in the L_1 norm and in the integral measure a vertex of the unit simplex is the optimal perturbation, and in the L_1 norm a vertex is also the perturbation resulting in minimal growth at time t. However, this property that the perturbation of minimal growth is at a vertex is not shared by the integral measure in which because of cancelation that may occur if the propagator has entries of both signs, a perturbation with zero growth can exist which is not associated with a vertex of the unit simplex.

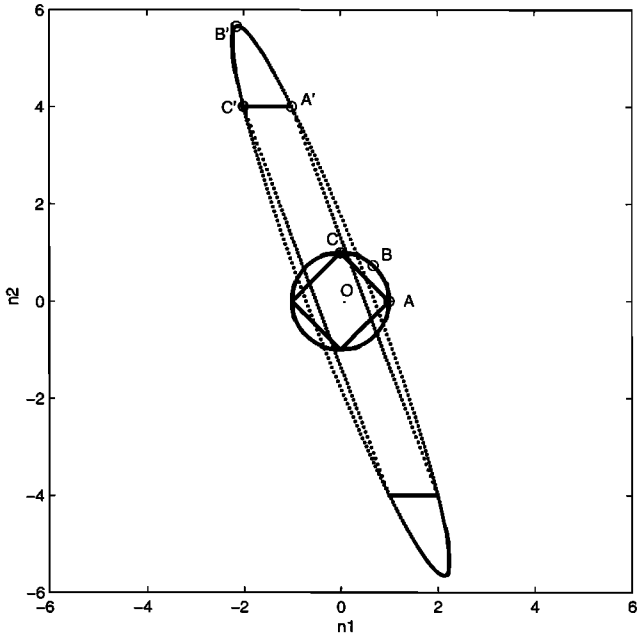

Figure 12. The result of applying the model 2×2 propagator (equation (A3)) to unit vectors in L_2 (the circle) and to unit vectors in L_1 (inscribed square). The optimal vector in L_2 is **OB**, which is mapped to the evolved optimal coincident with the semimajor axis **OB′** of length 6.05, leading to $||\mathbf{\Phi}||_2 = \mathbf{6.05}$. The optimal vector in L_1 is **OC**, and the L_1 norm of the evolved optimal, **OC′**, is $||\mathbf{\Phi}||_1 = \mathbf{6}$. The optimal vector in integral measure is **OA**, and it is mapped to the evolved optimal **OA′** with integral measure $[\mathbf{\Phi}] = \mathbf{3}$.

Appendix B: Optimal L_1 Excitations in the Asymptotic Limits

Consider first the $t \to \infty$ limit. We anticipate that every perturbation will assume the structure of the least damped mode in this limit. A similarity transformation diagonalizes the propagator: $e^{\mathbf{A}t} = \mathbf{U}\,\mathbf{D}\,\mathbf{U}^{-1}$, where $\mathbf{U}$ is the column matrix of the eigenvectors ordered according to $\mathrm{Re}(\lambda)$, where λ is the eigenvalue of the corresponding eigenvector, and $\mathbf{D}$ is the diagonal matrix with elements $e^{\lambda t}$. For large time the first diagonal element of $\mathbf{D}$ will exponentially dominate, so that with exponential accuracy we obtain

$$||e^{\mathbf{A}t}|| = e^{\mathrm{Re}(\lambda_1)t} \max_j \left[\left| \left(U^{-1}\right)_{1j} \right| \right] \left| \sum_i^N U_{i1} \right| , \quad \text{(B1)}$$

where λ_1 is the eigenvalue of the least damped mode, U_{i1} denotes an element of the eigenvector of the least damped mode which we wish to optimally excite, and $\left[\left(U^{-1}\right)^T\right]_{j1}$ are the elements of its bi-orthogonal. The optimal excitation is seen to occur for a delta function at the location of the maximum absolute amplitude of the bi-orthogonal rather than at the maximum of the mode itself as might have been anticipated. This result contrasts with the optimal excitation of the least damped mode in the L_2 norm. In that case the bi-orthogonal of the least damped mode itself optimally excites the mode [*Farrell and Ioannou*, 1996a]. If eigenanalysis of $\mathbf{A}$ is not feasible, the optimal excitation of the least damped mode can be identified as the dominant vector in the limit $t \to \infty$ in the transposed system, which is the bi-orthogonal of the least damped mode.

In the $t \to 0$ limit the appropriate problem is to determine the initial perturbation, $\mathbf{n}$, of unit L_1 norm that leads to maximum instantaneous growth rate in the integral measure. This is given by

$$g = \lim_{t\to 0} \frac{||e^{\mathbf{A}t}|| - 1}{t} = \lim_{t\to 0} \frac{||\mathbf{I} + \mathbf{A}t|| - 1}{t}, \quad \text{(B2)}$$

the second equality is obtained by Taylor expanding the propagator. The maximum growth rate is, in general, the maximum absolute sum obtained by a column of $\mathbf{A}$, and the perturbation that produces it is the canonical basis vector at the column of $\mathbf{A}$ corresponding to this maximum column sum (note that this is different from $||\mathbf{A}||_1$, which is the maximum obtained by a sum of absolute values of the columns of $\mathbf{A}$).

We may also obtain the perturbation that instantaneously grows most rapidly in the L_1 norm. An analysis similar to that above leads to the result that this maximum growth rate is the maximum sum of the columns of the matrix with elements

$$C_{ij} = \begin{cases} |A_{ij}| & i \neq j \\ A_{ij} & i = j, \end{cases} \quad \text{(B3)}$$

and the perturbation that produces it is the canonical basis vector that corresponds to the column of $\mathbf{C}$ with the maximum column sum (note that this is again different from $||\mathbf{A}||_1$, unless all elements of $\mathbf{A}$ are positive). In the L_1 norm we can also determine the perturbation that leads to the minimum instantaneous growth rate: this perturbation is corresponding to the column of $\mathbf{C}$ with minimum column sum of absolute values.

Appendix C: Mean and Variance of the Statistical Steady State

C1. Continual Stochastic Forcing

Consider the response to continual stochastic forcing. Assuming $n_i(0) = 0$, the forced response at time t is

$$n_i(t) = \int_0^t e_{ij}^{\mathbf{A}(t-s)}\, W_{jk}\, p_k(s)\, ds\,, \quad \text{(C1)}$$

where the propagator is $e^{\mathbf{A}t}$, $\mathbf{W}$ is the structure matrix of the forcing, and the vector forcings are considered to be white noise in space and time, i.e., $< p_k(t) p_l(s) >= \delta_{kl}\delta(t-s)$. The central limit theorem implies that the distribution of the evolved vector $n_i(t)$ approaches normal with mean at time t:

$$\bar{n}_i(t) = \left(\int_0^t e_{ij}^{\mathbf{A}(t-s)}\, W_{jk}\, ds \right) \bar{p}_k\,, \quad \text{(C2)}$$

which as $t \to \infty$ becomes

$$\bar{n}_i(\infty) = -\, A_{ij}^{-1}\, W_{jk}\, \bar{p}_k\,. \quad \text{(C3)}$$

The variance of $n_i(t)$ at each level can be obtained from the matrix

$$\mathbf{C}^t = \int_0^t e^{\mathbf{A}(t-s)}\, \mathbf{W}^i\, \mathbf{W}^{iT}\, e^{\mathbf{A}^T(t-s)}\, ds, \quad \text{(C4)}$$

which satisfies the Lyapunov equation [*Farrell and Ioannou*, 1996a]

$$\mathbf{A}\,\mathbf{C}^\infty + \mathbf{C}^\infty\,\mathbf{A}^T = -\,\mathbf{W}^i\,\mathbf{W}^{iT}\,, \quad \text{(C5)}$$

asymptotically as $t \to \infty$. The long time variance of n_i is C_{ii}^∞. Knowing the mean and the variance of n_i permits calculation of all statistical moments. An equivalent alternative view proceeds from Fourier analysis of the dynamical system to obtain the stochastic frequency response [*Farrell and Ioannou*, 1996a].

C2. Response to Impulsive Introduction of an Ensemble of Initial Perturbations

Consider now the expected growth of an ensemble of initial perturbations, $\mathbf{n}(0)$. The central limit theorem implies that the distribution of the evolved vector $n_i(t) = \sum_{j=1}^N \Phi_{ij}(t)\, n_j(0)$ approaches normal with mean:

$$\bar{n}_i(0) = \sum_{j=1}^N \Phi_{ij}(t)\, \bar{n}_j(0), \quad \text{(C6)}$$

where $\overline{n}_j(0)$ is the mean of the ensemble of the initial perturbations at the jth grid and $\Phi(t)$ is the propagator

at time t. The variance at each level i is given by

$$\sigma_i^2 = \sum_{j=1}^{N} \Phi_{ij}^2(t) \; < n_j^2(0) >, \qquad \text{(C7)}$$

where $< n_j^2(0) >$ are the variances of the initial perturbations. Knowing the mean and the variance of $n_i(t)$ permits calculation of the expected value of $< |n_i(t)| >$ in closed form:

$$< |n_i(t)| > = \sqrt{\frac{2}{\pi}}\, \sigma_i \, \exp\left(-\frac{\overline{n}_i(t)^2}{2\sigma_i^2}\right) + + \overline{n}_i(t) \, \mathrm{erf}\left(\frac{\overline{n}_i(t)}{\sqrt{2}\sigma_i}\right), \qquad \text{(C8)}$$

and consequently the expected growth of an ensemble of initial conditions is given in the L_1 norm by

$$< ||\mathbf{n}(t)||_1 > = \sum_{i=1}^{N} < |n_i(t)| > . \qquad \text{(C9)}$$

Appendix D: Effect of Nonnormality on Reservoir Turnover Time

We show that the turnover time defined in (21) depends on the nonnormality of $\mathbf{A}$. Consider the simple 2×2 system matrix:

$$\mathbf{A}(t) = \begin{pmatrix} -0.1 & 10 \\ 0 & -0.2 \end{pmatrix}, \qquad \text{(D1)}$$

representing in a schematic form the processes of advection and dissipation. This matrix is nonnormal and the reservoir turnover time for a source at the first grid is easily found to be 10, i.e., $||-\mathbf{A}^{-1}[1,0]^T||_1 = 10$, while for a source at the second grid the reservoir turnover time is 505, i.e., $||-\mathbf{A}^{-1}[0,1]^T||_1 = 505$. The corresponding turnover times for the diagonal normal matrix with the same eigenvalues are 10 and 5. So two systems with the same decay rates of their natural modes possesses vastly different reservoir turnover times. This demonstrates that the reservoir turnover times can be importantly affected by the nonnormality of $\mathbf{A}$.

Acknowledgments. The authors wish to acknowledge discussions with Denise Mauzerall, Larry Horowitz, and Steve Wofsy.

References

Andrews, D. G., J. R. Holton, and C. B. Leovy, *Middle Atmospheric Dynamics*, Academic, San Diego, Calif., 1987.

Chameides, W. L., and E. M. Perdue, *Biogeochemical Cycles*, Oxford Univ. Press, New York, 1997.

Farrell, B. F., Optimal excitation of perturbations in viscous shear flow, *Phy. Fluids*, *31*, 2093-2102, 1988.

Farrell, B. F., and P. J. Ioannou, Generalized stability, part I, Autonomous operators, *J. Atmos. Sci.*, *53*, 2025-2040, 1996a.

Farrell, B. F., and P. J. Ioannou, Generalized stability, part II, Non autonomous operators, *J. Atmos. Sci.*, *53*, 2041-2053, 1996b.

Golub, G. H., and C. F. Van Loan, *Matrix Computations*, Johns Hopkins Univ. Press, Baltimore, Md., 1996.

Khalil, M. A. K., and R. A. Rasmussen, Modeling chemical transports and mass balances in the atmosphere, in *Environmental Exposure From Chemicals, Vol. 2*, edited by W. B. Neely and G. E. Blau, CRC Press, Boca Raton, Fla., 1984.

Prather, M. J., Timescales in atmospheric chemistry: theory, GWPs for CH_4 and CO, and runaway growth, *Geophys. Res. Lett.*, *23*, 2597-2600, 1996.

Prather, M. J., Timescales in atmospheric chemistry: CH_3Br, the ocean, and ozone depletion potentials, *Global Biogeochem. Cycles*, *11*, 393-400, 1997.

Prather, M. J., Timescales in atmospheric chemistry: Coupled perturbations N_2O, NO_y, and O_3, *Science*, *279*, 1339-1341, 1998.

Trefethen, L. N., Pseudospectra of matrices, in *Numerical Analysis*, edited by D.F. Griffiths and G. A. Watson, pp. 234-266, Addison-Wesley-Longman, Reading, Mass., 1991.

B. Farrell, Department of Earth and Planetary Sciences, Harvard University, 29 Oxford Street, Cambridge, MA 02138. (farrell@io.harvard.edu)

P. Ioannou, Section of Astrophysics, Astronomy and Mechanics, Department of Physics, National and Capodistrian University of Athens, Zografos 15784, Athens, Greece. (pji@cc.uoa.gr)

(Received August 26, 1998; revised September 29, 1999; accepted September 30, 1999.)